



Published in final edited form as:

Methods Mol Biol. 2019 ; 2037: 151–168. doi:10.1007/978-1-4939-9690-2_9.

Stable Isotope Resolved Metabolomics by NMR

Penghui Lin¹, Andrew N. Lane^{1,2}, Teresa W-M Fan^{1,2}

¹Center for Environmental and Systems Biochemistry, University of Kentucky, Lee T. Todd Jr. Building, 789 S. Limestone St., Lexington, KY 40536

²Department of Toxicology and Cancer Biology, University of Kentucky, Lee T. Todd Jr. Building, 789 S. Limestone St., Lexington, KY 40536

Abstract

Stable isotopes enable the tracing of atoms from precursors to products via metabolic transformations in situ and in crude extracts. NMR has some unique capabilities that are especially suited for metabolic analysis, including atom position-resolved isotope analysis and isotope editing. In this chapter we describe NMR-based analysis of positional isotopomer distribution using metabolic tracers

Keywords

Stable Isotope Resolved Metabolomics; isotopomers; spectral editing; quantification

1. Introduction

Metabolic activity is both quantitatively and qualitatively specific to tissue and cell types, and is generally highly responsive to changes in external (environmental) or internal (e.g. genetic) perturbations. Thus cellular metabolism provides a very rich and molecular readout of the functional state of cells [2]. In metabolic research, stable isotope tracing provides much more rigorous metabolic pathway details than total metabolite profiling, as it can help resolve which intersecting pathways are active, and be used for estimating network fluxes [1–4].

For stable isotope tracing, there are two main analytical approaches that are widely applied, mass spectrometry (MS) and NMR. Although NMR is much less sensitive than most MS detection methods, it has several unique advantages for metabolite analysis. These are (i) quantification without the need for authentic standards; (ii) reliable quantitation with high dynamic ranges; (iii) ability to elucidate molecular structures with multidimensional and multinuclear capabilities; (iv) ability to determine distributions of labeled atom position(s), i.e. isotopomers; (v) isotope editing capabilities for spectral simplification in complex mixtures.

The goal of this chapter is to provide detailed experimental procedures for NMR identification and quantification of metabolites and their isotopomer distributions in Stable Isotope-Resolved Metabolomics (SIRM) studies. It should be noted that the experiments and analyses can be used for those with or without stable isotope enrichment.

The sensitivity of an NMR experiment is determined primarily by the amount (concentration) of each analyte and the nature of the detector system, primarily the probe type and magnetic field strength. Sensitivity theoretically scales as $B_0^{1.5}$, though in practice it is closer to linear in B_0 especially for the now prevalent cryoprobes. Cryoprobes may yield a sensitivity enhancement of 3–4 fold compared with an RT probe counterpart, which corresponds to about 10-fold reduction in experimental time for a given signal-to-noise ratio (SNR). However, this may be optimistic for salty samples, and the loss of sensitivity due to the presence of mobile ions increases with increasing magnetic field strength. The salt-associated losses however are somewhat offset by using smaller diameter microprobes, such as 3 mm or 1.7 mm compared with the “standard” 5 mm probe. When samples are severely limited, such as for tissue biopsy, microprobes outperform standard diameter probes. Routine high-resolution 5 mm cryoprobes at 16.45–18.8 Tesla typically have and SNR of 6000–8000:1 for 0.1% ethyl benzene in CDCl_3 . This translates to an SNR of 10:1 in 10 minutes acquisition (for a 6 s recycle time) in 1D ^1H NMR experiments for a volume of 300 μL at 0.5 nmol for each analyte in a Shigemi tube with optimal shimming and probe tuning.

2. Materials

1. *Cell or tissue extracts, biofluids.* Cells and tissue can be extracted simultaneously into fractions containing polar and non-polar (lipids) metabolites, respectively [5, 6]. Polar extracts are best lyophilized to minimize metabolite degradation during drying process. Lipid extracts can be evaporated under vacuum centrifugation or N_2 purge. If lipid extracts can be lyophilized if they contain excess water.
2. After lyophilization, the polar residue is best redissolved in 99.9% D_2O (or higher grade) or in a buffer in D_2O , preferably low in paramagnetic impurities. An external standard such as DSS- d_6 (e.g. 0.5 mM) is added to serve both as a chemical shift reference standard and as a concentration reference, which should be prepared as accurately as possible by weighing. For optimal referencing and quantification, the DSS concentration should be sufficiently high but not excessively higher than those of the metabolites of interests, due to consideration for the dynamic range of signal digitization. We have been using 18–27.5 nmoles of DSS- d_6 per 55 μL of D_2O for our extracts.

We find that dissolving extracts in D_2O will suffice in providing NMR spectra with consistent chemical shifts for most biological samples, as the extract pHs do not vary significantly. This avoids adding buffer salts to the extract. A common aqueous buffer for reconstituting polar extracts is 50 mM sodium phosphate in D_2O buffered to pD 7. For tissue extracts or extracts with high levels of paramagnetic ions such as Fe^{3+} , it is advisable to include 1 mM or higher EDTA- d_{12} to minimize line-broadening effects.

3. The non-polar extracts after drying can be dissolved in either d_4 -methanol or $CDCl_3$. The chemical shift references can be the residual proton resonance of the solvent. For quantification, an internal standard (e.g. trimethylsilane or TMS) must be added at a known amount.
4. For biofluids such as blood plasma, CSF or urine, it is possible to perform NMR analysis without processing other than dilution with a strong buffer to normalize the pH. Biofluids are typically very salty, which can compromise sensitivity of cryoprobes at high magnetic field strengths. Biofluids also contain high concentrations of protein and lipid, which interfere with quantification, particularly for 1H spectroscopy, as they produce broad overlapping peaks that make accurate peak integration problematic. Techniques for suppressing the broad resonances are available but they also differentially affect the intensities of the sharper metabolite resonances. Furthermore, the intense water resonance needs to be suppressed, and several suppression techniques either obliterate a large region of the spectrum, leading to loss of information and/or produce spectral artefacts (see below).
5. An alternative is to extract biofluids using a suitable solvent (e.g. 80% acetone) [7] to remove proteins and lipids, followed by reconstitution as described above for cells and tissues in step 1.
6. Samples should be centrifuged before use to remove particulates that may negatively impact shims and thus sensitivity and resolution.

3. NMR Methods

3.1 General setup

1. Add an appropriate amount of DSS-containing buffer to lyophilized samples depending on the length of the sensing region in the NMR probe. A typical amount is 35–55 μL for 1.7 mm tubes, 120–200 μL for 3 mm tubes and 300–500 μL for 5 mm Shigemi tubes. Make sure that the samples are completely dissolved by rigorous vortexing and removed of particulates by centrifugation at 20,000xg for 5 min before transferring to the NMR tubes.
2. Load sample into the magnet from the top opening or via an autosampler. If possible, samples in the autosampler should be cooled to $-10\text{ }^\circ C$ to better maintain sample integrity during prolonged runs.
3. Regulate the sample temperature using the instrument controls. Allow at least 2 min for temperature to stabilize before any NMR experiment. We find that $15\text{ }^\circ C$ is a good compromise between optimal spectral quality and reduced sample deterioration.
4. Tune the probe by switching the ‘tune’ and ‘match’ knobs under the probe or through the autotune and automatch feature (if available). The tune and match capacitors are not independent thus both must be adjusted iteratively for optimal

result. Make sure that the resonance curve is centered on the reference frequency with least reflection (deepest curve).

5. Select appropriate solvent and lock the sample. Adjust the lock power, gain and phase for optimal lock signal. Typically the lock level should be set around 50–60 %.
6. Shim the sample. Typically, use a representative sample of the whole set for shim optimization. Start by loading the last best shim file from the system, adjust z1, z2 and radial shims for the best lock signal. Then apply gradient shimming routine with an appropriate shim map for optimal gradient shims. In the ^1H spectrum of a well shimmed sample, the linewidth at half height of DSS methyl resonance should be less than 1 Hz and the silicon satellite peaks should be well resolved (i.e. <12 Hz at 2.3% height, since $^2J_{\text{H-Si}}$ is ca. 6 Hz and the ^{29}Si natural abundance is 4.67%, which gives a pair of satellites of about 2.3 % on either side of the methyl resonance).
7. Set the carrier frequency for proton to be on resonance with water peak, if water suppression is needed [8]. This is achieved by obtaining a test ^1H spectrum without water suppression (typically one scan with very small flip angle or excitation pulse width and receiver gain set at very low level to avoid signal saturation). Locate the water peak center and read the offset frequency value. Set this value as the transmitter carrier frequency offset for the presaturation experiment.
8. All experiments are run without sample spinning.

3.2. Specific experimental setup

3.2.1. Presat (^1H) experiment

1. Calibrate the 90-degree excitation pulse width of proton precisely for each set of samples for best quantification. Typically setting the transmitter power to the lowest while keeping the ^1H pulse width under 10 μs is optimal.
2. Select the water presaturation pulse sequence with the correct transmitter carrier frequency offset set from step 7 in **3.1** and the presaturation time set to 4 s for optimal water peak saturation. For a 99.9% D_2O sample, the water concentration is still about 55 mM, which is much higher than those of metabolites. Weak field presaturation with a field strength of ca. 20 Hz is sufficient to suppress the water signals. However, for samples with higher water content, a stronger rf field will be required (50 Hz or more).
3. Set the acquisition time to 2 second for achieving 0.5 Hz/point resolution in the raw free induction decay (FID) data. In this case, the total recycle time is 6 s, sufficient ($> 5 T_1$) to recover most of the metabolites' magnetization ($> 95\%$), since the T_1 of most small molecules are in the range of 1 s (cf. Notes 1,2 and Figure 3).

4. Use at least 8 dummy transients to achieve steady state. 256 + 8 dummy transients takes **26.4 minutes** of acquisition.
5. Process the FIDs with linear prediction once and zero-filling to four times of the original size. For example, 2-s acquisition with a spectral width of 12 ppm on a 14.1 T spectrometer results in 14368 complex points in the raw FID. Linear prediction once results in 32 k points, followed by zero filling to give 128 k points for a final resolution <0.1 Hz/point.
6. Apodize the FIDs with an exponential function that matches the natural half-height linewidth (e.g. 1 Hz) before Fourier transformation.
7. Adjust phase carefully, correct baseline using a third order Bernstein polynomial for accurate peak integration or deconvolution.
8. Reference the spectrum to DSS at 0 ppm.

3.2.2. 1D ^1H $\{^{13}\text{C}\}$ -HSQC—Compared to 1D ^1H experiments which detect all observable protons, HSQC detects the protons directly bonded to ^{13}C . It is a much more sensitive method for ^{13}C isotope detection than direct ^{13}C observation, which require much longer acquisition times due to the low gyromagnetic ratio of ^{13}C .

1. Tune the ^{13}C channel and carefully calibrate the ^{13}C pulse width using the first increment of the 2D HSQC experiment by maximizing the signal as a function of the INEPT delay.
2. Set proton carrier frequency on the HOD resonance the same way as step 7 in **3.1** if presaturation is desired.
3. The HSQC acquisition time is limited by the maximal ^1H decoupling time that the probe is allowed to prevent overheating, typically less than 250 ms.
4. Set spectral width to 12 ppm for the proton dimension and 200 ppm for the carbon dimension.
5. Apply adiabatic decoupling for broadband decoupling of carbons from protons. Set the coupling constant to the middle of the typical one-bond H-C coupling constant range (ca. 146 Hz), corresponding to a transfer delay of 3.425 ms ($1/2J$).

Presaturation may be applied during the relaxation time of 1.75 s giving a total cycle time of 2 s per transient. We typically acquire 1024 transients, which would need ca. **35 min.** of acquisition (cf. Note 3).
6. The FID is zero-filled to 16k data points, apodized with an unshifted half Gaussian (or cosine squared) function plus a 4 Hz exponential function, and Fourier-transformed.
7. Adjust the phase and correct the baseline, and reference the spectrum as described in steps 7,8, **3.2.1**.

3.2.3. 2D ^1H $\{^{13}\text{C}\}$ -HSQC—All setups are the same as the 1D ^1H $\{^{13}\text{C}\}$ -HSQC. Typical 2D HSQC setup includes a total of 64 real increments (128 total) in indirect carbon

dimension with 32 transients per increment. Under these conditions the experiment would take **2.3 h**.

3.2.4. High-resolution 2D ^1H $\{^{13}\text{C}\}$ -HSQC—The maximal spectral resolution in the proton dimension is set by the acquisition time, but that in the indirect carbon dimension can be adjusted.

1. Set the carrier frequency at 50 ppm and a spectral width of 120 ppm in the carbon dimension to span the entire aliphatic carbon region. Such spectral width reduction optimizes signal detection via efficient ^1H decoupling and resolution of ^{13}C - ^{13}C couplings in ^{13}C -enriched compounds via better digital resolution.
2. Set the increment in the indirect dimension to be 512 or more (real) with 32 transients per increment. Total experiment time is around **18 hours**.
3. For 2D data processing, linear predict FIDs once to 4096 and 1024 points in the ^1H and ^{13}C dimensions, followed by zero-filling to 8192 and 2048 data points respectively, apodization with an unshifted half Gaussian (or cosine squared) function plus an respective exponential line broadening function of 1 Hz in t_1 and 4 Hz in t_2 , and Fourier transformation. The final resolution in the indirect carbon dimension is 8.8 Hz/points, which is sufficient to resolve the one-bond ^{13}C - ^{13}C couplings of about 40 Hz.
4. Adjust the phases of the spectrum in F1 and F2, correct the baseplane and reference both dimensions to DSS at 0 ppm or to a known resonance at the proper chemical shift (e.g. the glucose 1- α resonance at 5.22 ppm for ^1H and 94.61 ppm for ^{13}C).

3.2.5. 1D ^1H $\{^{15}\text{N}\}$ -HSQC—Since ^{15}N has a natural abundance 0.37% and a gyromagnetic ratio of $1/10^{\text{th}}$ of the proton, it is not suitable for direct detection and therefore not a routine experiment for metabolite analysis. However, if metabolites are enriched in ^{15}N from labeled tracer precursors (e.g. ^{15}N -glutamine, -tryptophan, etc.), this experiment can provide direct evidence of nitrogen incorporation into metabolites at specific positions [1, 9] or for detection of ^{15}N -labeled metabolites via chemoselective derivatization using ^{15}N -labeled reagents [10, 11].

Typical one-bond NH coupling constants are around 90–95 Hz. However, most NHs are not detectable in proton spectra due to chemical exchange with water. If the proton to be detected is directly attached to ^{15}N such as in amides and peptides, the experiment must be carried out in $^1\text{H}_2\text{O}$ and for optimal signals at acidic pH (e.g. pH 4–5) and lower temperature (e.g. 10 °C) to minimize proton exchange. Multiple-bond NH coupling such as in a molecular fragment NCH may also be detected. Two-bond to three-bond NH coupling constants are in the range 1–5 Hz [10].

1. Set carrier frequencies at water resonance for proton dimension and 120 ppm for the nitrogen dimension (to cover both amide and non amide resonances) with spectral widths of 10 ppm and 50–60 ppm for proton and nitrogen dimensions, respectively.

2. Tune the ^{15}N channel and carefully calibrate the ^{15}N pulse width using the first increment of the HSQC experiment (cf Step 1 **3.2.2**).
3. Set the acquisition time in the proton dimension to be the same as the broadband decoupling duration, typically less than 250 ms. GARP decoupling is applied on the nitrogen dimension during acquisition. If carbon decoupling is also desired, it can be applied simultaneously during acquisition.
4. Apply a very weak soft pulse presaturation during the relaxation time if needed. For 1024 + 8 steady state transients the experimental time is **34 minutes**.
5. Zero-fill the final FID to 16 K data points, apodize with unshifted half Gaussian (or cosine squared) function plus 4 Hz exponential line-broadening before Fourier transformation.
6. Adjust phase, reference, and correct baseline as in step 7, **3.2.1**.

3.2.6. 2D ^1H $\{^{15}\text{N}\}$ -HSQC—All setups are identical to the 1D $^1\text{H}\{^{15}\text{N}\}$ HSQC experiment.

1. A typical setup includes 64 increments in the indirect dimension with 32 transients per increment, which amounts to approximately **2.3 h** total acquisition time.
2. Process the 2D data, adjust phase, baseplane correct and reference the spectrum as described in step 4, **3.2.4**.

3.2.7. High-resolution 2D ^1H $\{^{15}\text{N}\}$ -HSQC—As in 2D $^1\text{H}\{^{13}\text{C}\}$ HSQC, resolution in the proton dimension is limited by the decoupling time allowed by the probe, but the resolution in the indirect ^{15}N dimension can be adjusted as desired.

1. Set the total number of increments in the indirect dimension to 512 over a 60 ppm spectral width. With 32 transients per increment, the total experiment time is around **9 h**.
2. Linear predict FIDs once with one zero filling before apodization and Fourier transformation as in step 3, **3.2.4**. This provides the digital resolution in the ^{15}N dimension to be around 1.7 Hz/point, sufficient to resolve ^1H - ^{15}N one and two-bond couplings of 8–16 Hz [13, 14].
3. Process the 2D data, adjust phase, baseline correct and reference the spectrum as described in step 4, **3.2.4**. ^{15}N shifts can be referenced indirectly according to [12]

3.2.8. TOCSY (Total Correlation Spectroscopy)—This experiment correlates scalar coupled spins in the entire spin systems.

1. Set the offset of proton carrier frequency at HOD resonance determined by 1D PRESAT experiment (ca. 4.8 ppm at 20 °C).

2. Set the spectral widths to 10 ppm (e.g. -0.2 to 9.8 ppm) in both dimensions for samples in D_2O unless the 1D spectrum shows resonances outside this range.
3. Set the acquisition and relaxation delay times in the direct dimension (t_2) to 1 s.
4. Apply solvent suppression the same way as in the PRESAT 1D 1H experiment in 3.2 and apply soft pulse presaturation during relaxation time.
5. Set the isotropic mixing spinlock time to 50 ms via the MLEV17 or DIPSI-2 pulse sequence. This duration enables magnetization relay for up to 4 bonds, thereby providing up to 4 covalent bond correlations in the molecular structure, which is sufficient for small metabolites.
6. Calibrate the B_1 field strength to deliver 8–10 kHz for the spin lock
7. Apply magnetic gradients with a zero quantum filter to obtain better quality spectra.
8. Set 4096 real points and 256 real increments in the direct (t_2) and indirect (t_1) dimensions, respectively. Determine the number of transients according to the sample concentration. Typical samples use 16 transients per increment with 256 real increments, which amounts to total experimental time of **4.6 h**.
9. Zero-fill FIDs to a final matrix of 8192×1024 real data points, apodize with an unshifted half Gaussian (or cosine squared) function plus a 1 Hz exponential function, and Fourier transform in both dimensions.
10. Process the 2D data, adjust phase, baseline correct and reference the spectrum as described in step 4, 3.2.4 except that both spectral dimensions are referenced to DSS at 0 ppm.

3.2.9. Double-quantum filtered COSY (DQ-COSY)—This is a pure phase COSY experiment that detects scalar coupling between protons 2–4 bonds apart.

1. Set offset of proton carrier frequency to the HOD resonance determined by the 1D PRESAT experiment.
2. Set the spectral width to 10 ppm in both dimensions, acquisition times of 1 s in t_2 , 256 real (512 total) increments in t_1 , and a relaxation delay of 1 s with solvent suppression as needed. For 16 transients per increment, this requires **4.6 h** of experimental time (cf. Note 4).
3. Process the 2D data, adjust phase, baseline correct and reference the spectrum as described in step 10, 3.2.8.

3.2.10. Heteronuclear multiple bond correlation spectroscopy (HMBC)—This experiment complements HSQC as it detects X- 1H correlations over 2–4 bonds, with coupling constants typically in the range of 1–4 Hz. It can therefore detect non-protiated atoms such as quaternary ^{13}C or ^{15}N or ^{13}C carbonyl groups.

1. Set proton carrier frequency for the HOD resonance determined by 1D PRESAT experiment and the ^{13}C carrier offset to 100 ppm

2. Set the spectral widths to 10 ppm in the ^1H and 200 ppm in the ^{13}C dimensions
3. Optimize the HMBC delay in a 1D experiment to assess sensitivity over the range of couplings present (1–4 Hz). This will determine the effective J values used for the evolution time.
4. Set 4096 real points and 128 real increments (256 total) in the proton and carbon dimensions, respectively with a recycle time of 1.5 s. For 64 transients per increment, the experimental time is **6.8 h** (cf. Note 5).
5. Process the 2D data, adjust phase, baseline correct and reference the spectrum as described in step 4, **3.2.4**.

3.2.11. Other editing experiments.—NMR is exceptionally rich in the variety of experiments that can be performed, especially when NMR-active stable isotopes are present [4, 15–17]. In addition to the common experiments described above, other less utilized isotope-edited experiments are also valuable in providing complementary and cross-validating information on isotopomer distributions in labeled tracer studies.

1. **2D HNC0** This experiment must be carried out in $^1\text{H}_2\text{O}$ and requires both ^{15}N and ^{13}C enrichment in metabolites to detect protons attached to ^{15}N alpha to a ^{13}C carbonyl group. ^{15}N must be enriched to a high level. For amides, this is best carried out at pH 4 and lower temperature (e.g. 10 °C) to minimize proton exchange. The experiment can be carried out either as $^1\text{H}^{13}\text{C}$ plane or $^1\text{H}^{15}\text{N}$ plane. The HC plane is especially useful, which requires only a small number of increments due to a narrow spectral width (ca. 20 ppm centered at 180 ppm). For 32 real increments with 32 transients per increment, the experimental time per plane is ca. **68 min**.
2. **HCCH TOCSY** This experiment detects protons attached to consecutively ^{13}C enriched carbons. The experimental setup is similar to TOCSY with spectral widths of 10 ppm in both ^1H dimensions, real increments of 256, and recycle time of 2 s. Typically, with 32 transients per increment requires a total experiment time of **9 h**.
3. **HSQC TOCSY** This experiment detects coupling of X nucleus to directly bonded protons and protons that are 2–4 bonds away. The acquisition conditions are otherwise the same as individual HSQC and TOCSY experiments as described above.

4.3. Assessing sensitivity to determine experimental time needed

Most of the 2D experiments have maximal sensitivity in the first increment (DQ-COSY is an exception as it has no intensity in the first increment). Thus, it is useful to test spectral sensitivity by performing 1D experiment using the first increment.

1. Execute a 1D experiment with all of the optimized parameters for the first increment (for DQ-COSY, set the initial delay to 40 ms to assess sensitivity)

2. Assess the intensity of peaks that are desired for analysis, e.g. nucleotides, lactate, Ala, Glu, glutathione, etc. Although there is a 2D advantage in signal detection for the full 2D experiment, if the resonances are not visible in 1D spectra acquired with the first increment, they are unlikely to be visible in the 2D spectra (cf. Note 6)

3.3 NMR assignments

Processed NMR spectra can be assigned based on chemical shifts, covalent connectivity, and other NMR parameters as in [18–21]. Detailed assignment strategies are beyond the scope of this chapter.

4. Concentration determination

4.1. 1D NMR methods

Concentrations are determined from integrated peak areas, **A** as follows [1, 6].

$$A = k \cdot c \cdot n \cdot f$$

where **c** is the concentration of the compound

n is the number of equivalent protons in the resonance (e.g. 3 for a methyl, 2 for a methylene and 1 for a methine)

f is the saturation factor (cf. Note 8)

k is an undetermined proportionality constant that depends on the spectrometer and settings

Suppose there are two compounds, 1 and 2, then

$$A_1/A_2 = c_1 f_1 n_1 / c_2 f_2 n_2$$

$$c_1 = c_2 (A_1/A_2) (f_2 n_2 / f_1 n_1)$$

If **c**₂ is known, then **c**₁ can be determined.

The expected error in **c**₁ is then (assuming no covariance):

$$|dc_1/c_1| = dc_2/c_2 + dA_2/A_2 + df_2/f_2 + dA_2/A_2 + df_1/f_1$$

For well-resolved peaks, with good SNR (>10:1), the errors in area determination should be <10%.

The procedure for concentration determination by 1D NMR is as follows.

1. Determine the peak areas by integration or peak deconvolution including the methyl protons of the DSS standard and their ²⁹Si satellites (Note 7)

2. Determine the number of protons for a given resonance to be quantified, e.g. 9 for DSS methyl protons; 1–3 for CH, CH₂, CH₃, respectively for most metabolites).
3. Determine the f values based on the experimental setup. R_1 can be determined by using the fast inversion recovery pulse sequence for the particular samples or set of samples in the same matrix (cf. Note 8).

4.2. 2D NMR methods

Volume integration can be performed using the 3D version of the trapezoidal rule, which has shown to be reliable when the digitization in both dimensions is adequate [22].

4.2.1. Volume integration using the VNMRJ software

1. Linear predict, zero-fill, apodize, and Fourier transform 2D data; phase, reference, and baseplane correct, as described above.
2. Set $ins2ref = 1$, $ins2 = 1e6$ to $1e8$
3. choose region of interest (RoI)
 - ll2d('clear')
 - ll2d('peak', 'pos') – selects positive peaks in the RoI
 - ll2d('adjust', 'volume')
 - ll2d('writetext', 'filename')
4. The text file includes peak volumes (v) corresponding to picked peaks and RoI selected
5. Paste peak volumes with the assignments into an excel file (cf. Note 9).

4.2.2. Volume integration using the MestReNova software

1. Load FID data into the MestReNova software. Process each spectrum as described above including linear prediction, zero filling, phase adjustment, referencing, and baseline correction if applicable.
2. For volume quantification of 2D NMR spectra, MestReNova provides two different tools: peak picking and integration.
3. For 2D spectral peak picking, two different options can be used, “Manual Threshold” and “Peak by Peak”. In manual threshold mode, drag the mouse over the area to be picked, the MestReNova algorithm will automatically detect the contours under a predefined threshold and fit the contour with deconvolution. In “Peak by Peak” mode, the mouse drag will jump from point to point on the highest point of each contour. Clicking the mouse will pick the contour where the peak point sits. However, in this mode the deconvolution will not be applied.
4. In the peak-picking mode, all peak information can be directly exported to an Excel file including chemical shifts, height, linewidth, volume, etc.

5. For 2D integration, MestReNova also provides several tools: automatic integration, predefined region integration, and manual integration. In the automatic integration mode, a 2D peak-picking algorithm will be applied in the background, so it is essentially the same as using the 2D peak picking methods with deconvolution. In the predefined region integration mode, the user can set up the regions of interest for the software to integrate instead of the whole spectrum. More importantly, these regions can be saved and applied to the next spectrum, which is very useful for metabolomics analysis as the same metabolites are usually analyzed across a large number of samples. In manual integration mode, the user can click and drag with the mouse to select the region to be integrated. The first integral will be normalized to 1.0 and all following integrals will be referenced to the first one. The absolute values can be found in the integral tables generated by MestReNova. These tables are also readily exported into excel files (cf. Note 10).

5. Isotopomer distribution analysis

5.1. 1D ¹H NMR analysis

Isotopomers of given metabolites are always present due to natural abundance of ¹³C (1.1 %) and ¹⁵N (0.37 %). These can be observed (with low sensitivity) by direct detection methods or by the appearance of satellite peaks in the proton spectrum. In the case of ¹³C satellites, there are two doublet resonances spaced equally on either side of the resonance of ¹H attached to ¹²C (Fig 1, top spectrum), with intensities of about 0.55%. In ¹³C₆-glucose labeling experiments, the satellite peaks are more complex and increase in relative intensity (Fig. 1, bottom spectrum). The absolute and fractional enrichment can be readily quantified from such spectrum as follows.

1. Process 1D ¹H spectra as described in 3.2.1.
2. Integrate (cf. Note 7) the ¹²C-¹H peak and its two satellites
3. Correct for partial saturation using measured T₁ values (cf. Note 8), if needed.
3. calculate the fraction ¹³C at this site as:

$$F = A(^{13}\text{C})/[A(^{13}\text{C}) + A(^{12}\text{C})]$$

5. Assign the isotopomer from the fine splitting pattern (e.g. ¹³C₃ lactate or ¹³C_{1,2,3}-lactate for example).

5.2. 2D ¹H NMR analysis

2D ¹H TOCSY spectra are recorded and processed as described above (Section 3.2.8). Figure 2 shows the spectral region where the cross-peaks for Asp and Glu and their ¹³C satellites occur. The isotopomer distribution can be analyzed as follows.

1. Volume integrate (cf. 5.2) all of the components of the cross peaks, including their fine structure [22].
2. Identify the ¹²C¹²C cross-peaks

3. Identify the $^{13}\text{C}^{12}\text{C}$ and $^{13}\text{C}^{13}\text{C}$ cross-peaks and add volumes of all related peaks (see Figure 2) to obtain v_{sat}
4. Sum the volumes of all of the cross-peak components to obtain v_{tot}
5. Calculate the mole fraction of each component as

$$F = v_{\text{sat}}/v_{\text{tot}}$$

6. Notes

Note 1. NOESY 1D with water presaturation [23] and Excitation Sculpting [24] methods may also be applied for proton spectroscopy where the solvent is predominantly $^1\text{H}_2\text{O}$. The advantage of using NOESY1D is that it eliminates most of the macromolecule signals to provide a cleaner baseline whereas water sculpting method suppresses the water peak better. However, NOESY1D tends to suppress a larger bandwidth in which metabolite signals close to water are also suppressed (e.g. glucose and oxidized glutathione), leading to inaccurate quantification. Excitation sculpting results in phase distortion in the peaks that is impractical to phase, which also lead to inaccurate quantification.

Note 2. The number of transients or scans can be determined by the signals from the peaks of interests. In general, 512 transients would result in **52 min acquisition**, which provides sufficient SNR for most peaks while limiting the experimental time to a reasonable scale. If the SNR is not adequate with one hour of data acquisition, it may not worth investing more experimental time for detection. As SNR increases with the square root of the number of acquisitions, e.g. to increase the SNR from 5:1 to 10:1 would increase the acquisition time from 1 h to 4 h.

Note 3. Under these settings, most protons will be partially saturated and saturation correction needs to be made based on T_1 values of each proton group.

Note 4: For cell extracts with ca. 1 mg total solutes, this is a usually the minimal time for analysis. As the cross-peak multiplets are in antiphase, the peak volumes can be underrepresented, so DQ-COSY is not well-suited for quantitative isotopomer analysis.

Note 5: The HMBC is significantly less sensitive than the HSQC experiment due to T_2 relaxation during the longer delays and spreading signals over multiple resonances.

Note 6: If sufficient sensitivity is not reached in 64–96 transients, then one should increase the sample concentration or seek measurement on a higher sensitivity instrument.

Note 7: There are several methods to integrate peaks in NMR spectra and all require accurate phase adjustment and good baselines. The standard integration method, based on the trapezoidal rule, is very accurate if the baseline is properly adjusted and there is no significant overlap. It is tolerant of unresolved couplings, imprecise shimming, and thus lineshape distortions (which may occur in automated runs). An alternative method is line shape fitting, which performs an iterative non-linear regression to a mixture of Lorentzian and Gaussian line shapes, and can thus deconvolute overlapping peaks. In software packages

like MestReNova (<http://mestrelab.com/software/mnova/>), lineshape fitting can be semi-automated and run in a batch mode. However, it is sensitive to deviations from Lorentzian/Gaussian lineshapes and unresolved couplings. The Chenomx software (<https://www.chenomx.com/>) uses proprietary libraries of experimentally derived peak shapes of metabolites for sequential curve fitting and spectral subtraction, which can detect obscured metabolite signals but is very time-consuming.

Note 8: Partially saturated peak intensity can be corrected by obtaining the saturation factor (f) where $f = 1/(1-\exp(-R_1D))$

R_1 is the spin-lattice relaxation rate constant ($=1/T_1$) and D is the experimental recycle time, i.e. acquisition time + relaxation delay for a PRESAT experiment. f values for different relaxation rate constants for three different recycle times are shown in Figure 3.

The DSS methyl resonance has a short R_1 value (ca. 0.3 s^{-1}), which corresponds to an underestimated peak area by up to 20% without correction, and thus a corresponding underestimated concentration).

The other source of error arises from uncertainty in c_2

Note that the analysis of peak areas, saturation factors, and reference concentration should be accurate to better than 1 % to achieve an estimate error of 1–2 % for c_2 determination.

Errors accruing from inaccuracies in T_1 determination have been treated in [25].

Also note that protons attached to ^{13}C will relax faster than those attached to ^{12}C , and thus the T_1 values for the satellite peak must also be measured [26].

Note 9. Integration of empty regions of the spectrum should also be done and subtracted from the estimated volumes.

Note 10. Peak volume integration in MestReNova is defined as the sum of all digital intensities within the footprint (integration area or RoI). The footprint shape can be set to rectangular or elliptical. In low-resolution spectra with no significant fine peak structure, the elliptical RoI is superior. However, in higher resolution spectra where multiplet fine structures are resolved and need to be independently integrated, the rectangular footprint may be more accurate..

Acknowledgments

This work was supported in part by NIH grants 1U24DK097215-01A1, CA163223-01A1, 5P20GM121327 (COBRE) the Carmen L. Buck endowment (to ANL), and the Edith D. Gardner Chair in Cancer Research (TWMF).

Abbreviations:

DSS	2,2-Dimethyl-2-silapentane-5-sulfonate
FID	free induction decay rf radiofrequency
RoI	region of interest

SIRM	Stable Isotope Resolved Metabolomics
SNR	signal to noise ratio
TMS	trimethylsilane

References

1. Fan TW-M and Lane AN, Applications of NMR to Systems Biochemistry. *Prog. NMR Spectrosc.*, 2016 92: p. 18–53.
2. Lane AN and Fan TW-M, NMR-based Stable Isotope Resolved Metabolomics in systems biochemistry. *Arch. Biochem. Biophys.*, 2017 628: p. 123–131. [PubMed: 28263717]
3. Bruntz RC, Higashi RM, Lane AN and Fan TW-M, Exploring Cancer Metabolism using Stable Isotope Resolved Metabolomics (SIRM). *J. Biol. Chem.*, 2017 292: p. 11601–11609. [PubMed: 28592486]
4. Fan TW-M and Lane AN, NMR-based stable isotope resolved metabolomics in systems biochemistry. *Journal of biomolecular NMR*, 2011 49(3–4): p. 267–280. [PubMed: 21350847]
5. Fan TW, Considerations of Sample Preparation for Metabolomics Investigation. *Handbook of Metabolomics*, 2012 17(17).
6. Fan TW-M and Lane AN, Assignment strategies for NMR resonances in metabolomics research, in *Methodologies for Metabolomics: Experimental Strategies and Techniques*, Lutz N, Sweedler JV, and Weevers RA, Editors. 2013, Cambridge University Press: Cambridge.
7. Fan TW, Warmoes MO, Sun Q, Song H, Turchan-Cholewo J, Martin JT, Mahan A, Higashi RM and Lane AN, Distinctly perturbed metabolic networks underlie differential tumor tissue damages induced by immune modulator beta-glucan in a two-case ex vivo non-small-cell lung cancer study. *Cold Spring Harb Mol Case Stud.*, 2016 2(4): p. a000893. [PubMed: 27551682]
8. Giraudeau P, Silvestre V and Akoka S, Optimizing water suppression for quantitative NMR-based metabolomics: a tutorial review. *Metabolomics*, 2015 11: p. 1041–1055.
9. Fan TW-M and Lane AN, NMR-based Stable Isotope Resolved Metabolomics in Systems Biochemistry. *J. Biomolec. NMR* 2011 49 p. 267–280
10. Lane AN, Arumugam S, Lorkiewicz PK, Higashi RM, Laulhe S, Nantz MH, Moseley HNB and Fan TW-M, Chemoselective detection of carbonyl compounds in metabolite mixtures by NMR. *Mag. Res. Chem.*, 2014 53: p. 337–343.
11. Tayyari F, Gowda G, Gu H and Raftery D, 15N-cholamine--a smart isotope tag for combining NMR- and MS-based metabolite profiling. *Anal Chem.*, 2013 85: p. 8715–8721. [PubMed: 23930664]
12. Wishart DS, Bigam CG, Yao J, Abildgaard F, Dyson HJ, Oldfield E, Markley JL and Sykes BD, 1H, 13C and 15N chemical shift referencing in biomolecular NMR. *Journal of Biomolecular NMR*, 1995 6(2): p. 135–140. [PubMed: 8589602]
13. Heikkinen S, Permi P and Kilpeläinen I, Methods for the Measurement of 1JNCA and 2JNCA from a Simplified 2D 13Ca-Coupled 15N SE-HSQC Spectrum. *J.Magnetic Resonance* 2001 148: p. 53–60.
14. Niu C, Bertrand RD, Shindo H and Cohen JS, Cross-peptide bond 13C--15N coupling constants by 13C and J cross-polarization 15N NMR. *J Biochem Biophys Methods*, 1979 1(3): p. 135–43. [PubMed: 552384]
15. Clore GM and Gronenborn AM, NMR structure determination of proteins and protein complexes larger than 20 kDa. *Current Opinion in Chemical Biology*, 1998 2(5): p. 564–570. [PubMed: 9818180]
16. Otting G and Wuthrich K, Heteronuclear Filters In 2-Dimensional H-1, H-1 Nmr-Spectroscopy - Combined Use With Isotope Labeling For Studies Of Macromolecular Conformation and Intermolecular Interactions. *Quarterly Reviews of Biophysics*, 1990 23(1): p. 39–96. [PubMed: 2160666]

17. Gardner KH and Kay LE, The use of H-2, C-13, N-15 multidimensional NMR to study the structure and dynamics of proteins. *Annual Review of Biophysics and Biomolecular Structure*, 1998 27: p. 357–406.
18. Fan TW-M and Lane AN, Assignment strategies for NMR resonances in metabolomics research, in *Methodologies for Metabolomics: Experimental Strategies and Techniques*, Lutz N, Sweedler JV, and Wevers RA, Editors. 2013, Cambridge University Press: Cambridge p. 525.
19. Fan TW-M, Metabolite profiling by one- and two-dimensional NMR analysis of complex mixtures. *Progress in Nuclear Magnetic Resonance Spectroscopy*, 1996 28: p. 161–219.
20. Fan TW-M and Lane AN, Structure-based profiling of Metabolites and Isotopomers by NMR. *Progress in NMR Spectroscopy*, 2008 52: p. 69–117.
21. Fan TW and Lane AN, Applications of NMR spectroscopy to systems biochemistry. *Prog Nucl Magn Reson Spectrosc*, 2016 92–93: p. 18–53.
22. Lane AN and Fan TW, Quantification and identification of isotopomer distributions of metabolites in crude cell extracts using 1H TOCSY. *Metabolomics*, 2007 3: p. 79–86.
23. Le Guennec A, Tayyari F and Edison AS, Alternatives to Nuclear Overhauser Enhancement Spectroscopy Presat and Carr–Purcell–Meiboom–Gill Presat for NMR-Based Metabolomics. *Anal. Chem*, 2017 89: p. 8582–8588. [PubMed: 28737383]
24. Hwang TL and Shaka AJ, Water Suppression That Works. Excitation Sculpting Using Arbitrary Wave-Forms and Pulsed-Field Gradients. *Journal of Magnetic Resonance, Series A*, 1995 112: p. 275–279.
25. Lane AN, NMR applications in metabolomics in *Handbook of Metabolomics*, Fan TW-M, Lane AN, and Higashi RM, Editors. 2012, Humana.
26. Lane AN, Fan TW and Higashi RM, Isotopomer-based metabolomic analysis by NMR and mass spectrometry. *Biophysical Tools for Biologists.*, 2008 84: p. 541–588.

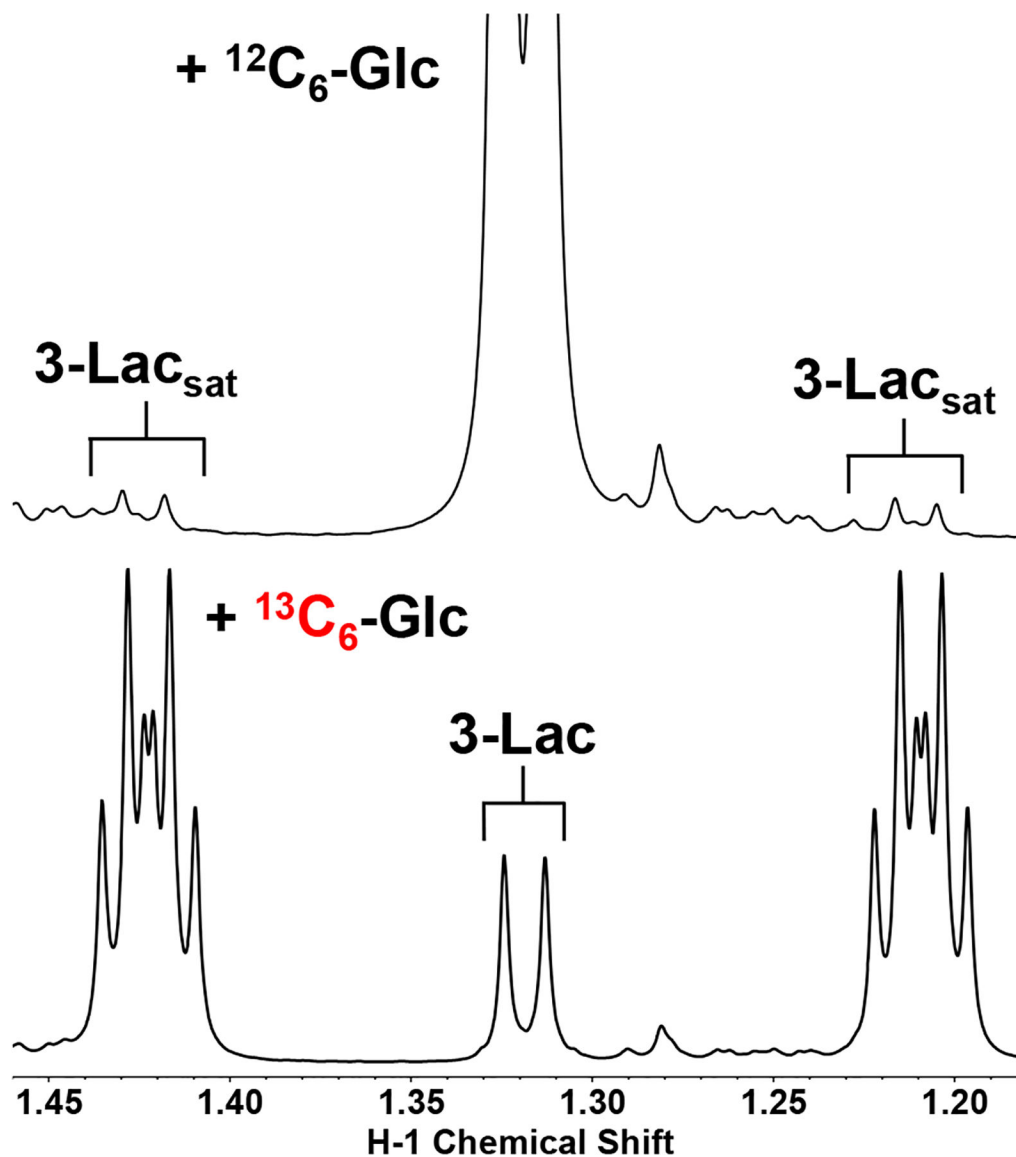


Figure 1. 1D Presat spectrum of medium extracts from human macrophage cultures. Polarized human macrophages were grown in the presence of unlabeled ($^{12}\text{C}_6\text{-Glc}$) or $^{13}\text{C}_6\text{-glucose}$ for 24 h. The lactate (Lac) methyl resonance of protons attached to ^{12}C occurs at 1.32 ppm in both spectra. The two ^{13}C satellite (Lac_{sat}) peaks display as a pair of doublets in the natural abundance spectrum (top) and as a pair of multiplets in the labeled spectrum (bottom). The multiplets comprise 6 peaks each due to coupling to the $^{13}\text{C}_2\text{H}$, $^{13}\text{C}_2$, and $^{13}\text{C}_3$, showing that this lactate isotopomer is $^{13}\text{C}_{1,2,3}$ [1]. The fraction (F) of ^{13}C enrichment is determined to be 0.90.

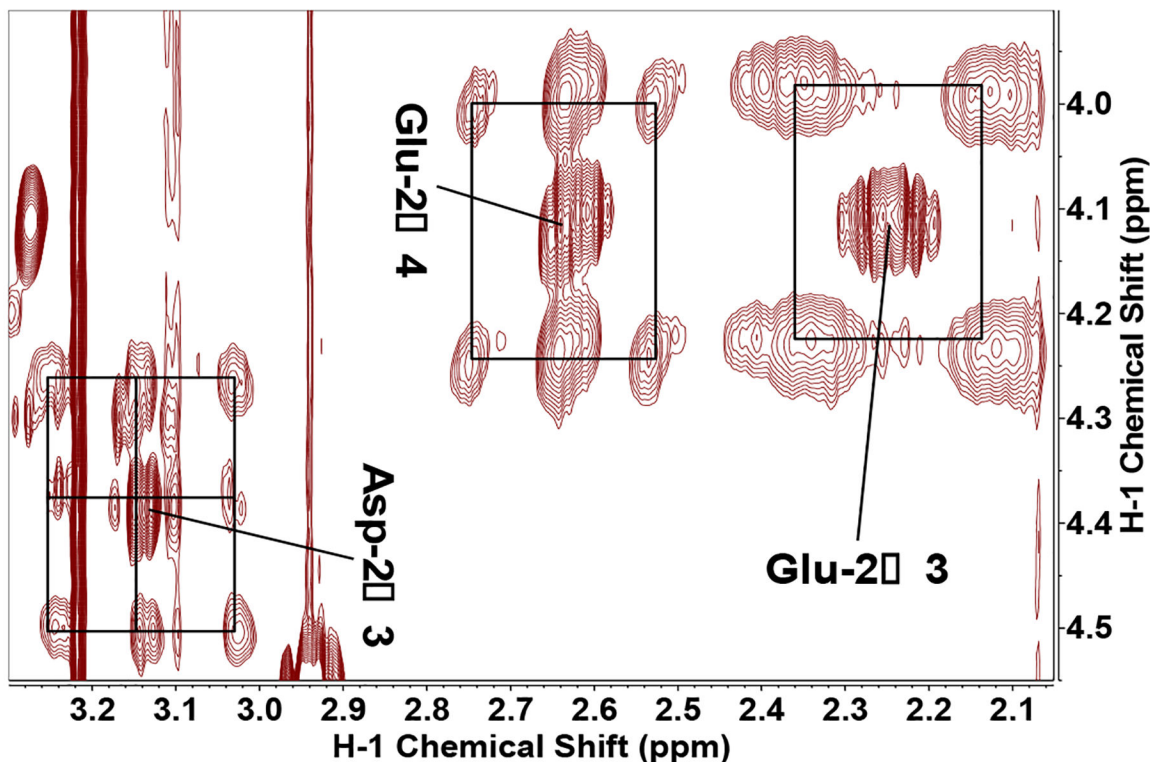


Figure 2. 2D ^1H TOCSY spectrum of a cancer cell extract.

MCF7 breast cancer cells were grown in the $^{13}\text{C}_5$ -Gln and unlabeled glucose for 24 hr. The ^1H TOCSY spectrum was acquired at 14.1 T for the cell extract. The spectral region where cross-peaks from Asp and Glu occur is shown. The annotated central cross-peaks correspond to protons attached to ^{12}C . The surrounding satellite peaks (delineated by boxes) arise from protons attached to ^{13}C . For the Asp 2 \rightarrow 3 cross-peak, there are 4 satellite peaks corresponding to the isotopomers $^{13}\text{C}_2^{13}\text{C}_3$, two peaks for $^{13}\text{C}_2^{12}\text{C}_3$ and two for $^{12}\text{C}_2^{13}\text{C}_3$. The Glu2 \rightarrow 4 and Glu2 \rightarrow 3 cross-peaks show only 4 satellites respectively for $^{13}\text{C}_2^{13}\text{C}_4$ and $^{13}\text{C}_2^{13}\text{C}_3$.

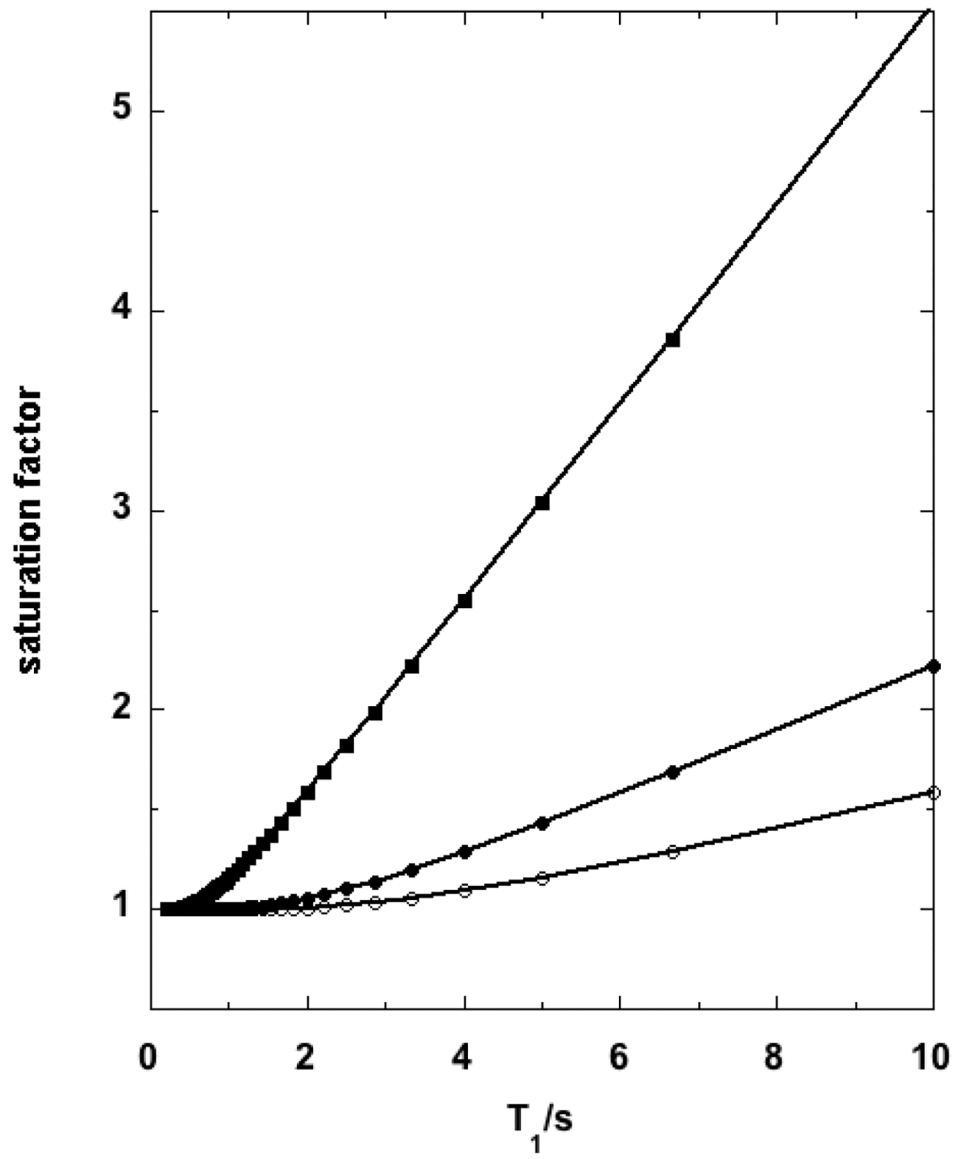


Figure 3. Saturation factors versus T_1 values for three different recycle times. Saturation factors were calculated using $f = 1/(1-\exp-R_1D)$ with $D=2$ s (■), 6 s (●) and 10 s (○)